JPP Journal of Pharmacy and Pharmacology

JPP 2007, 59: 1077–1085

Received February 6, 2007
Accepted May 8, 2007
DOI 10.1211/jpp.59.8.0004
ISSN 0022-3573

Central nervous system distribution kinetics of indinavir in rats

Mehrdad Hamidi

Abstract

The central nervous system (CNS) distribution kinetics of indinavir were extensively evaluated using a combinational in-vivo model comprising the integration plot method (a single-passage approach) and neuropharmacokinetic method (a multiple-passage approach). A 5 mg kg^{-1} dose of indinavir was administered intravenously to rats. Blood and cerebrospinal fluid (CSF) samples and whole brain were collected from the animals at specified time points and the drug concentration in each sample was determined using a high-performance liquid chromatography method. For the neuropharmacokinetic study, the simultaneous plasma, CSF and brain concentrations were fitted to an integrated model, which resulted in the estimation of the influx (K_{in}) and efflux (K_{out}) rate constants of the drug to/from CSF and brain parenchyma. The integration plot method involved plotting the brain–plasma or CSF–plasma concentration ratios ($K_{p,app}$) against $AUC_{0\rightarrow t}/C_{p(t)}$, and estimating the uptake clearance of the drug by brain/CSF from the slope of the initial linear portion of the plot. The K_{in} and K_{out} values of the drug to/from CSF were estimated to be 2.42×10^{-2} and 13.26×10^{-2} min^{-1}, respectively, and the corresponding values for brain parenchyma were 1.02×10^{-2} and 1.32×10^{-2} min^{-1}, respectively. The uptake clearances of indinavir by CSF and brain parenchyma were 8.89 and 8.38 $\mu L\,min^{-1}\,g^{-1}$, respectively. The permeability surface area products of the drug for the blood–brain barrier and blood–CSF barrier were estimated as 1.05×10^{-2} and 2.45×10^{-2} $mL\,min^{-1}\,g^{-1}$, respectively. The estimated kinetic parameters indicated limited CNS entry of the drug because of the limited blood–brain barrier permeability and the efficient drug efflux from CNS, particularly from CSF.

Introduction

Since the identification of human immunodeficiency virus type 1 (HIV) as the causative agent for acquired immunodeficiency syndrome (AIDS), a series of central nervous system (CNS) symptoms, including numerous cognitive and motor skill deficiencies, collectively referred to as AIDS dementia complex, have been designated as concurrent with progressive immune system failure due to the HIV infection (e.g. Krebs et al 2000). In addition, the CNS has been described as an immunological sanctuary site with the potential to act as a viral reservoir (Pialoux et al 1997; Erickson et al 1999).

The development of HIV protease inhibitors was a major advance in the clinical management of HIV infection and their use as a part of combinational highly active antiretroviral treatment regimens has resulted in dramatic reductions in viral load in the plasma and many tissues of infected patients (Eron 2000). However, several studies have reported that the CNS distribution of HIV protease inhibitors is highly restricted (Kim et al 1998; Choo et al 2000; Haas et al 2000; Megard et al 2002), thereby limiting the therapeutic efficacy of these drugs in the CNS (Krebs et al 2000). The limited CNS penetration of HIV protease inhibitors is mainly attributed to the expression of P-glycoprotein (P-gp) in the blood–brain barrier (BBB) (Kim et al 1998; Lee et al 1998; Choo et al 2000; Megard et al 2002). P-gp, a 170-KDa glycoprotein product of the multidrug resistance gene, is a member of the ATP-binding cassette superfamily of transporters and is involved in the active efflux of a wide variety of compounds, including pharmacologically active agents from the CNS (Tatsuta et al 1992). In addition to P-gp, there is some evidence from an in-vitro study supporting the role of multidrug resistance-associated protein in the limited CNS distribution of HIV protease inhibitors (van der Sandt et al 2001).

Department of Pharmaceutics, Faculty of Pharmacy, Shiraz University of Medical Sciences, PO Box 71345-1583, Shiraz, Iran

Mehrdad Hamidi

Correspondence: Mehrdad Hamidi, Department of Pharmaceutics, Faculty of Pharmacy, Shiraz University of Medical Sciences, PO Box 71345-1583, Shiraz, Iran.
E-mail: hamidim@sums.ac.ir

Acknowledgement: The initial phase of this study was carried out in the Faculty of Pharmacy, University of Toronto, Canada. The author wishes to thank Ahmadreza Mehdipour for his assistance with the preparation of this manuscript.

Indinavir is a potent HIV protease inhibitor with favourable virological, immunological and clinical characteristics (e.g. Gulick et al 1997). Concentration dependency has been demonstrated for the anti-HIV activity of indinavir (Acosta et al 1999). Suboptimal concentrations of the drug in the CNS lead to therapeutic failure as well as the emergence of drug-resistant viral strains, despite the adequate plasma concentrations and acceptable systemic antiviral efficacy indicators (Pialoux et al 1997; Erickson et al 1999). At present, there is limited in-vivo data on the CNS distribution of indinavir (Kim et al 1998; Martin et al 1999; Choo et al 2000; Haas et al 2000; Megard et al 2002). In some of these studies (Kim et al 1998; Choo et al 2000; Megard et al 2002), radiolabelled drug was administered to the animals, followed by measurement of the total radioactivity recovered in the brain at a single or a limited number of time points. These studies suffer from the possibility of the occurrence of metabolite interference, particularly considering that the drug has extensive species-specific in-vivo metabolism, with *N*-dealkylation, *N*-oxidation and hydroxylation reactions being more remarkable in rat, all mediated by CYP3A4, a microsomal enzyme with extensive tissue distribution throughout the body (Lin et al 1996; Chiba et al 1997, 2000), as well as the limited number of time points at which the tissue radioactivity recovery was measured. Another set of studies (Martin et al 1999; Haas et al 2000) involved measurement of the simultaneous serum and cerebrospinal fluid (CSF) drug concentrations in HIV-infected patients during the steady state of drug therapy. These studies cannot provide direct information about the BBB permeability of indinavir because the drug concentration in CSF does not necessarily reflect the extent to which the drug is able to cross the BBB. The purpose of the present study was to characterize the transport kinetics of indinavir in the CNS using a combinational in-vivo model comprising a single-passage approach that estimates the CNS uptake clearance of the drug using the plasma and tissue concentrations determined during the early time period of drug exposure, and a multiple-passage approach that estimates the CNS influx and efflux rate constants of the drug using the tissue and plasma concentrations throughout the full-course drug pharmacokinetic study.

Materials and Methods

Materials

Indinavir sulfate (ethanol solvate form, MW 757.9) was kindly donated by Merck Research Laboratories (Rahway, NJ, USA). Verapamil hydrochloride (racemate form), triethylamine, phosphoric acid (assay 85.3%), and *tert*-butyl methyl ether were purchased from Sigma-Aldrich Canada Ltd (Oakville, ON, Canada). Perchloric acid (assay 70%) was purchased from BDH Inc. (Toronto, ON, Canada). High-performance liquid chromatography grade water and acetonitrile were purchased from Caledon Laboratories Ltd (Georgetown, ON, Canada). All other reagents used were of analytical grade and were prepared locally.

Animals

Male Sprague–Dawley rats (Charles River, St Constant, Quebec, Canada), 280–300 g, were used in this study. The animals were kept in standard cages with free access to water and standard rat chow. A 12-h day/night cycle was used, with lights on at 0800 hours. The protocol for the animal experiments was reviewed and approved by the University of Toronto Animal Care Committee. The animals were cared for in accordance with the guidelines of the Canadian Council on Animal Care. All the animal experiments were carried out in the Faculty of Pharmacy, University of Toronto, Canada.

Plasma protein binding

In order to determine the unbound fraction of indinavir in rat plasma over the plasma concentration range expected in this study, spiked samples with final nominal concentrations of 0.5, 2.0, 8.0, and 16.0 μM were prepared by the addition of appropriate solutions of the drug in ethanol in a volume fraction of 2% to the rat blank plasma. The pooled freshly obtained plasma sample withdrawn by cardiac puncture from four rats was used for spiked sample preparation and, after incubating 1-mL samples at 37°C for 30 min, a 0.5-mL portion of each sample was centrifuged using a Microcon YM-10 centrifugal ultrafiltration device (Millipore, Danvers, MA, USA) at 10 000 *g* and 37°C for 30 min. While this portion was being centrifuged, the remainder of each sample (0.5 mL) was kept incubated for another 30 min. The resulting filtrate was kept frozen at −70°C until the drug assay time, together with the unfiltered part. The experiment was performed in triplicate and, for each concentration, the unbound fraction of the drug was determined by dividing the drug concentration in the filtrate by that of the corresponding unfiltered portion. A series of drug solutions in phosphate buffer (pH 7.4) with the same concentrations as the spiked plasma samples were prepared and processed as described for determination of the possible binding of indinavir to the ultrafiltration filter or device.

Drug administration

The day before the experiments, the rats were anaesthetized by intraperitoneal injection of a ketamine/xylazine cocktail (ketamine 100 mg kg^{-1} and xylazine 10 mg kg^{-1}) and a polyethylene/silicone rubber cannula was implanted in the right jugular vein according to a standard method (Waynforth & Flecknell 1992). The rats were kept singly overnight to recover. On the day of the experiments, a 5-mg kg^{-1} dose of indinavir sulfate (6.6 μmol) dissolved in a saline/propylene glycol/ethanol vehicle (5:4:1, v/v/v; 5 mg mL^{-1}) was injected into each rat through the cannula. The animals remained unrestrained during the entire drug administration and sampling time. At 1, 5, 10, 30, 60, 120, 180, 240, 360 and 420 min following the drug administration, the animals were anaesthetized by injection of an anaesthetic cocktail (ketamine 10 mg kg^{-1} and xylazine 1 mg kg^{-1}) via the cannula. Then, a 0.1-mL sample of CSF was withdrawn by direct cisternal puncture (Waynforth & Flecknell 1992) using a 25-G needle connected to a 1-mL syringe. Immediately after CSF sampling, a 0.5-mL blood sample was withdrawn from the cannula into a pre-heparinized polypropylene microtube. The animals were then decapitated and the brains were removed. A total of 40 rats were used to collect four replicate biological

samples at each time point. The plasma was separated by centrifuging the blood samples at 1000 *g* for 10 min and the brain was washed with 1 mL saline. The CSF, plasma and brain samples were kept frozen at −70°C until the drug assay time.

Drug assay

A simple and highly sensitive reversed-phase high-performance liquid chromatography method was developed (Hamidi 2006a) and used for the determination of indinavir concentrations in rat biological samples. The whole brains of rats were weighed (1.86 ± 0.23 g) and homogenized using a Teflon/glass homogenizer (Caframo, model 57022 Clamp; Wiarton, ON, Canada) while suspended in 2 mL saline. For drug analysis, to 500 μL of the brain homogenates or 100 μL of plasma samples, 100 or 20 μL of perchloric acid (70%) was added, respectively, and, after vortex mixing for 1 min, the resulting suspension was centrifuged at 18 000 *g* for 10 min. To 100 μL of CSF or 100 μL of plasma precipitation supernatant or 300 μL of brain homogenate precipitation supernatant, prepared as described, 20 μL of verapamil hydrochloride (internal standard) aqueous solution (15 μM), 1 mL of KOH 4 M solution and 3 mL of *tert*-butyl methyl ether were added and the resulting mixture was orbitally shaken at 1800 rev min^{-1} for 15 min and then centrifuged at 5000 *g* for 10 min. The organic layer was separated by aspiration into a clean 13-mL polypropylene test tube and evaporated to dryness using a vacuum centrifuge (Centrivap Console; Labconco Co., Kansas city, MO, USA) in ambient temperature. Finally, the dried sample was re-dissolved in 100 μL of phosphoric acid 100 mM solution and 50 μL of the resulting solution was injected onto the chromatograph. A mixture of phosphoric acid 50 mM aqueous solution and acetonitrile (65:35, v/v) with a final pH of 5.5, adjusted by the addition of triethylamine, was used as the mobile phase. The analyte separation was performed by a Synergi Hydro-RP column (150 × 4.6 mm, particle size 4 μm; Phenomenex Inc., Torrance, CA, USA) in ambient temperature. The eluent was delivered at a flow rate of 1.1 mL min^{-1} and the UV detection wavelength was 215 nm. The method produced linear responses over the concentration range of 0.05 to 30 μM of indinavir in plasma, and 0.05 to 2.5 μM in CSF and brain, with limits of detection of 12.5 nM for plasma and CSF, and 6.25 nM for brain homogenate. The average intra- and inter-run variations and accuracy of the method were 6.1%, 6.2% and 101.1% for plasma, 6.4%, 6.3% and 98.7% for brain homogenate and 8.1%, 5.9% and 100.6% for CSF, respectively. The recovery of indinavir and internal standard (verapamil) from all matrices tested was above 90%.

Plasma pharmacokinetics

Based on an initial visual inspection of the plasma concentration–time data, the pooled plasma concentration–time data from 40 rats were fitted to a standard biexponential decline equation using the non-linear regression fitter of SigmaPlot 5.0 software (SPSS Inc., Chicago, IL, USA):

$$C_{p(t)} = Ae^{-\alpha t} + Be^{-\beta t} \quad (1)$$

where $C_{p(t)}$ is the plasma concentration of indinavir at time t, A and B are intercepts and α and β are the slopes of the distribution and elimination regression lines, respectively. The curve fitting and parameter calculation steps were performed on both the total and unbound plasma concentration data, separately.

Neuropharmacokinetics

A method based on studies by Anderson et al (1990) and Galinsky et al (1990) was used for the estimation of the influx and efflux rate constants of indinavir to/from CSF and brain parenchyma in rat. The following assumptions were made for fitting the tissue concentration data to the neuropharmacokinetic model used in this study: (i) all the movements of the drug in the system (i.e. influx and efflux) are first order processes; (ii) there are no direct relationships between CSF and brain parenchyma in terms of the drug flux; (iii) both brain parenchyma and CSF are homogenous and well-mixed sampling compartments; (iv) there is no significant binding of the drug to the CNS components; (v) there are no sources for drug entry to brain parenchyma and CSF other than the circulating blood; and (vi) there are no compartments receiving the drug from CNS other than the circulating blood.

The rate of changes in indinavir concentration in brain parenchyma (dC_{par}/dt) can be expressed as:

$$dC_{par}/dt = K_{in}C_{p(t)} - K_{out}C_{par(t)} \quad (2)$$

where K_{in}, K_{out}, $C_{p(t)}$, and $C_{par(t)}$ represent the drug influx and efflux rate constants and plasma and brain parenchymal concentrations of indinavir at time t, respectively.

The concentration of drug in brain parenchyma is determined from the apparent total brain concentration by subtracting the drug concentration in the brain vascular space. Therefore, the drug concentrations measured in brain samples at time t ($C_{br(t)}$) relates to the brain parenchymal concentrations as:

$$C_{br(t)} = C_{par(t)} + (V_{vas}C_{p(t)}) \quad (3)$$

where V_{vas} is the fractional contribution of the volume of plasma content of brain vasculature in the whole brain volume.

Integration of Equation 2 using Laplace transformation, followed by replacing the corresponding value for $C_{p(t)}$ from Equation 1 and taking Equation 3 into account, yields:

$$C_{br(t)} = K_{in}\left[\frac{[A(\beta - K_{out}) + B(\alpha - K_{out})]e^{-K_{out}.t}}{(\alpha - K_{out})(\beta - K_{out})} + \frac{Ae^{-\alpha t}}{K_{out} - \alpha} + \frac{Be^{-\beta t}}{K_{out} - \beta}\right] + (V_{vas}C_{p(t)}) \quad (4)$$

Using a similar set of calculations, except for the inclusion of Equation 3, the following equation can be derived for the concentration of indinavir in CSF:

$$C_{CSF(t)} = K_{in}\left[\frac{[A(\beta - K_{out}) + B(\alpha - K_{out})]e^{-K_{out}.t}}{(\alpha - K_{out})(\beta - K_{out})} + \frac{Ae^{-\alpha t}}{K_{out} - \alpha} + \frac{Be^{-\beta t}}{K_{out} - \beta}\right] \quad (5)$$

where, analogous to Equation 4, K_{in} and K_{out} represent the drug influx and efflux rate constants from blood circulation to/from CSF, respectively. A diagrammatic representation of the pharmacokinetic model used in this study is shown in Figure 1.

Using the A, B, α and β values determined from plasma pharmacokinetic analysis described earlier, the pooled brain/CSF concentration–time data were fitted to Equations 4 and 5 using the non-linear regression fitter of SigmaPlot 5.0 software (SPSS Inc.) and the parameters K_{in}, K_{out} and V_{vas} were determined. In order to exploit the effect of plasma protein binding on the kinetic parameters determined, two sets of data fitting were performed separately using the pharmacokinetic parameters determined based on the unbound and total plasma concentrations of indinavir.

In order to evaluate the permeability characteristics of the drug across the BBB and blood–CSF barrier (BCSFB), the permeability–surface area product (PS) of indinavir was calculated for BBB and BCSFB using the K_{in} values for brain and CSF, respectively, according to the Renkin–Crone model of capillary transfer (Renkin 1959; Crone 1965):

$$K_{in} = \upsilon F\,(1 - e^{-PS/\upsilon F}) \quad (6)$$

where υF represents the cerebral plasma flow. The value for υF (0.578 mL min^{-1} g^{-1}) was calculated using the estimated rat global cerebral blood flow (GCBF) of 1.09 mL min^{-1} g^{-1} (Hagendorff et al 1994) and a hematocrit (HCT) value of 0.47 in rat (Waynforth & Flecknell 1992) as follows:

$$\upsilon F = GCBF\,(1 - HCT) \quad (7)$$

Graphic estimation of the uptake clearance

In order to determine the uptake clearance of indinavir by rat brain parenchyma and CSF, an integration plot method was used as described by Takasawa et al (1997a). The rate of change of the drug amount in a tissue ($dX_{(t)}/dt$) can be expressed as:

$$dX_{(t)}/dt = Cl_{uptake} \times C_{p(t)} \quad (8)$$

where, Cl_{uptake} represents the uptake clearance of the drug by the tissue.

Integration of Equation 8 yields:

$$X_{(t)} = Cl_{uptake} \times AUC_{0\to t} \quad (9)$$

where, $X_{(t)}$ is the amount of drug in the tissue at time t and $AUC_{0\to t}$ is the area under the plasma concentration–time curve from time 0 to t. Similar to what is specified in Equation 3 for drug concentrations in brain, the following relationship defines the total amount of drug per unit mass of the brain at time t ($X_{br(t)}$):

$$X_{br(t)} = X_{par(t)} + (V'_{vas} C_{p(t)}) \quad (10)$$

where $X_{par(t)}$ is the amount of drug per unit mass of the brain parenchyma at time t. V'_{vas} in Equation 10 is the volume occupied by the plasma in the brain vasculature per unit mass of the brain. Since the estimated specific gravity of brain is approximately 1 (Ohno et al 1978), the V'_{vas} in this equation can be considered equivalent to the V_{vas} included in Equation 3.

Equation 10 can be rewritten as:

$$X_{br(t)}/C_{p(t)} = Cl_{uptake} \times (AUC_{0\to t}/C_{p(t)}) + V_{vas} \quad (11)$$

Since the specific gravity of the brain is approximately 1 (Ohno et al 1978), the $X_{br(t)}$ and $X_{par(t)}$ values can be estimated by $C_{br(t)}$ and $C_{par(t)}$, respectively.

Using a similar set of calculations (except for the inclusion of V_{vas}), the following equation can be derived for CSF:

$$X_{CSF(t)}/C_{p(t)} = Cl_{uptake} \times (AUC_{0\to t}/C_{p(t)}) \quad (12)$$

Therefore, if the ratios of the drug concentrations in brain or CSF samples at time t to the simultaneous plasma concentrations ($K_{p,app}$) are plotted against the ratio of the $AUC_{0\to t}$ to the corresponding plasma concentrations ($AUC_{0\to t}/C_{p(t)}$), a linear relation is expected to be obtained at the early time intervals, with slope and y-intercept representing the apparent tissue uptake clearance and the fractional volume of plasma in brain vasculature, respectively (Takasawa et al 1997a).

The extraction ratios (ER) of indinavir by CSF and brain were determined using a classic equation (Shargel & Yu 1999):

$$ER = Cl_{uptake}/\upsilon F \quad (13)$$

Statistical methods

The pooled plasma/tissue concentration–time data in the full-course neuropharmacokinetic study from 40 rats was fitted to a standard biexponential decline equation using the non-linear regression fitter of SigmaPlot 5.0 software (SPSS Inc.). The linear regression analysis in the integration plot analysis

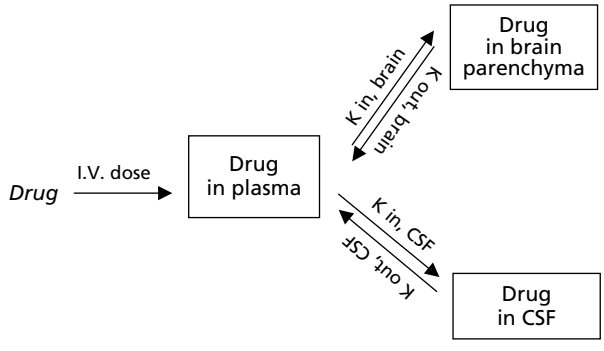

Figure 1 Pharmacokinetic model for central nervous system distribution of indinavir in rats. CSF, cerebrospinal fluid.

section was performed using Microsoft Excel 2003. The concentration dependency of protein binding was tested using the non-parametric Kruskal–Wallis test. The differences between two data groups in Table 2, when applicable as stated in the text, were tested by the non-parametric Mann–Whitney *U*-test. A level of $P < 0.05$ denoted significance in all cases.

Results

The total and unbound concentrations of indinavir upon incubation of different concentrations of the drug with rat plasma are listed in Table 1. The extent of indinavir protein binding was found to be concentration independent ($P > 0.05$) (mean unbound fraction of 47.8% ± 4.4). This binding behaviour has been reported previously for indinavir (Lin et al 1996). Therefore, the average unbound fraction of 47.8% was used for the calculation of unbound plasma concentrations from the corresponding total plasma concentrations. The average unbound fraction determined in this study is somewhat higher than the value of 30% previously reported in the same species (Lin et al 1996), which may be attributed to differences in the experimental conditions used (i.e. the filter type, volume of plasma tested, incubation period and centrifugation speed). The binding of indinavir to the ultrafiltration device was negligible at all concentrations tested (<1%).

The concentration–time profiles of indinavir in plasma (both total and unbound), CSF and brain parenchyma are shown in Figure 2. The relatively high distribution and elimination rate constants of indinavir (i.e. α and β values of about 50 min^{-1} and 3 h^{-1}, respectively) reflect a highly efficient disposition of the drug in this species, as previously reported by Lin et al (1996). The time courses of the ratios of drug concentrations in brain parenchyma and CSF to the corresponding plasma concentrations ($K_{p,app}$) are shown in Figure 3. The data indicate that there is a substantial difference between CSF and brain parenchyma in terms of the rate of equilibration of drug concentration with plasma concentrations. CSF seems to be a fast equilibrating tissue (i.e. central compartment), with a t_{max} of 5 min (Figure 2) and a relatively constant CSF-to-plasma concentration ratio after about 10 min (Figure 3), suggesting a high intra-tissue distribution rate (Figure 2). On the contrary, the brain parenchymal concentration shows a slow equilibration rate with the plasma concentration (i.e. peripheral compartment), with a low intra-tissue distribution rate reflected by a t_{max} of 60 min (Figure 2), and an ascending trend of the brain-to-plasma concentration ratio until 120 min (Figure 3).

Table 1 Indinavir protein binding in rat plasma

Nominal added concentration (μM)	Measured total concentration (μM)	Measured free concentration (μM)	Unbound fraction (%)
0.5	0.58 (0.03)	0.28 (0.02)	48.28
2.0	2.11 (0.14)	0.98 (0.08)	46.46
8.0	7.88 (0.75)	3.38 (0.34)	42.89
16.0	16.09 (1.03)	8.60 (0.88)	53.45
Mean (s.d.)			47.77 (4.40)

Data represent the mean (s.d.), n = 3.

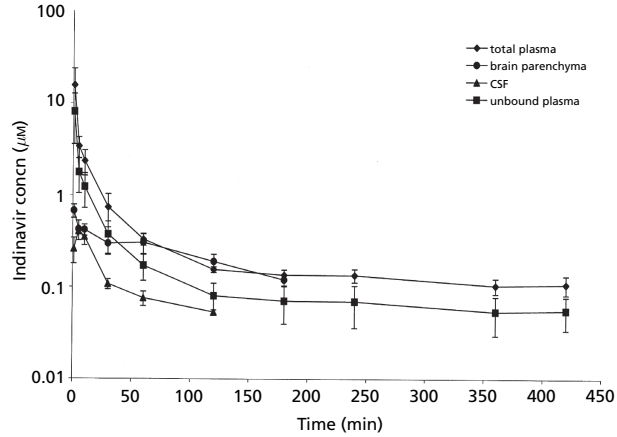

Figure 2 Plasma, brain parenchymal and cerebrospinal fluid (CSF) semi-log concentration–time profiles of indinavir after intravenous administration of 5 mg kg^{-1} indinavir sulfate to male Sprague–Dawley rats (n = 4 for each time point).

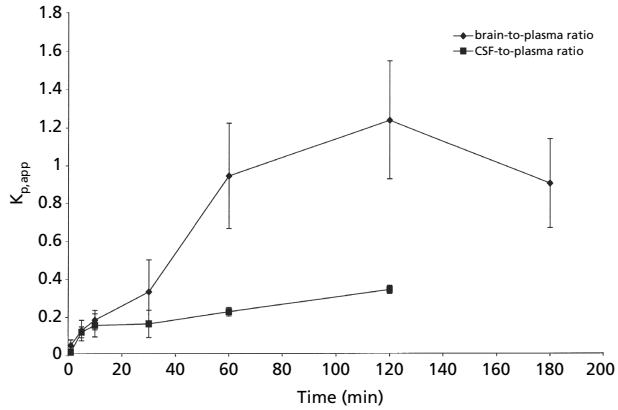

Figure 3 Brain parenchyma-to-plasma and cerebrospinal fluid (CSF)-to-plasma concentration ratios ($K_{p,app}$) of indinavir after intravenous administration of 5 mg kg^{-1} indinavir sulfate to male Sprague–Dawley rats (n = 4 for each time point).

As previously discussed, indinavir concentrations quantitated in brain samples (C_{br}) include both concentrations in brain parenchyma (C_{par}) and the contribution of the brain vasculature ($C_p V_{vas}$) (see Equation 3). In order to get a deeper insight into the CNS transport behaviour of indinavir, we used the V_{vas} value estimated by our neuropharmacokinetic analysis (Equation 4) to distinguish between the C_{br} and C_{par}. In fact, the concentration data shown in Figures 2 and 3 are parenchymal concentrations calculated from the corresponding measured brain and plasma concentrations using Equation 3.

The time courses of C_{br} and C_{par} are shown in Figure 4. These data indicate that, as expected, the contribution of the brain vasculature drug content in the measured brain concentrations is higher at the early time points. This may be explained by the highly efficient distribution and elimination

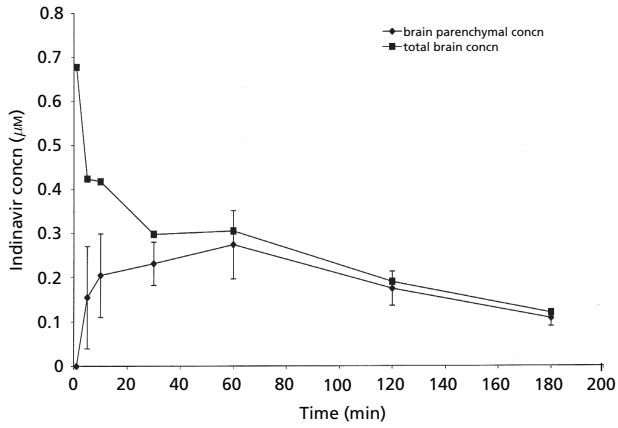

Figure 4 Brain total measured and parenchymal concentration–time profiles of indinavir after intravenous administration of 5 mg kg^{-1} indinavir sulfate to male Sprague–Dawley rats (n = 4 for each time point).

processes of the drug in this species (Figure 2), which in turn results in very low plasma concentrations after 60 min compared with the initial time points. The concentrations of indinavir in CSF and brain were undetectable in samples taken beyond the 120 and 180 min time points, respectively.

The CNS distribution kinetic parameters resulting from fitting the pooled CSF and brain concentration–time data of rats to Equations 4 and 5 are listed in Table 2. As predicted, the inclusion of two different sets of plasma pharmacokinetic parameters, estimated using the total and unbound plasma concentrations of indinavir, in our neuropharmacokinetic curve-fitting procedure resulted in a significantly different (approx. 2-fold) estimation of K_{in} (influx rate constant) values in the case of both CSF ($P < 0.01$) and brain ($P < 0.05$) data, whereas the K_{out} (efflux rate constant) values were not significantly different ($P > 0.05$ in both cases). Therefore, the plasma protein binding should be considered in the determination of tissue transport parameters using this model. While

Table 2 Neuropharmacokinetic parameters of indinavir in rats after the intravenous administration of 5 mg kg^{-1} indinavir sulfate to Sprague–Dawley rats (n = 4, for each time point)

Parameter	Brain	Cerebrospinal fluid
K_{in} (min^{-1})[a]	0.54×10^{-2} (7.92×10^{-4})[c]	1.26×10^{-2} (9.86×10^{-4})
K_{out} (min^{-1})[a]	1.31×10^{-2} (3.68×10^{-3})	13.01×10^{-2} (1.67×10^{-2})
K_{in} (min^{-1})[b]	1.02×10^{-2} (1.51×10^{-3})	2.42×10^{-2} (1.90×10^{-3})
K_{out} (min^{-1})[b]	1.32×10^{-2} (3.73×10^{-3})	13.26×10^{-2} (1.70×10^{-2})
V_{vas} (fractional)	0.06	NA
K_{out}/K_{in}[b]	1.28	5.50
Cl_{uptake} ($\mu L\ min^{-1}\ g^{-1}$)	8.38 (1.76)	8.89 (1.95)
V'_{vas} (fractional)[d]	0.09	NA
Extraction ratio	0.015	0.015

[a]Based on total plasma concentration of indinavir. [b]Based on free plasma concentration of indinavir. [c]Mean (s.e.). [d]Based on the initial uptake clearance data. NA, not applicable.

the estimated K_{in} and K_{out} values of the drug for brain parenchyma were not significantly different from each other ($P > 0.05$), the corresponding values for CSF were highly different ($P < 0.001$), which reflects a substantially more efficient efflux of the drug from CSF (K_{out}/K_{in} of 5.5; Table 2). The fractional volume of plasma content of the brain vasculature estimated by the neuropharmacokinetc data analysis (0.06; Table 2) is comparable with the values of 0.04 and 0.059 reported by Anderson et al (1990) and Galinsky et al (1990), applying the similar pharmacokinetic data analysis on 2′,3′-dideoxyinosine and zidovudine (AZT), respectively.

The apparent PS of indinavir for the BBB and BCSFB, estimated from Equation 6, were 1.05×10^{-2} and 2.45×10^{-2} mL min^{-1} g^{-1}, respectively. These values correspond to the permeability values of 6.77×10^{-5} cm min^{-1} and 3.27×10^{-4} cm min^{-1}, respectively, considering the reported surface areas of 155 and 75 cm^2 g^{-1} for the BBB and BCSFB, respectively, in rats (Keep & Jones 1990). These findings suggest greater (i.e. approx. 5 times) apparent permeability of the BCSFB for indinavir compared with the BBB and confirm the more "leaky" barrier structure of the BCSFB compared with the BBB (Fenstermacher et al 1981). Based on the permeability value of indinavir determined for the BBB, this drug can be considered to have relatively low BBB permeability compared with the permeability values determined in-vivo in rat for a series of about 20 compounds with diverse physicochemical properties (Pardridge et al 1990). The permeability value of indinavir for the BBB obtained in this study (i.e. 6.77×10^{-5} cm min^{-1}) is about 6-times greater than the corresponding value for [^{14}C]sucrose (1.05×10^{-5} cm min^{-1}; Pardridge et al 1990), a compound with one of the lowest brain permeability values reported so far.

Indinavir uptake clearance by rat brain parenchyma and CSF were estimated by applying an integration plot analysis as described by Takasawa et al (1997a). The integrated plots of indinavir brain-to-plasma and CSF-to-plasma concentration ratios ($K_{p,app}$) versus the ratio of the $AUC_{0 \rightarrow t}$ to the plasma concentration at time t following the intravenous administration of 5 mg kg^{-1} of the drug to rats are shown in Figure 5. As shown, the plots for both CSF and brain are linear at early time points up to 10 min. The initial linear portions of the plots were used for the estimation of the apparent uptake clearance of the drug by CSF and brain (Figure 5 inset). The linear regression analysis resulted in statistically acceptable r values for both sampling compartments (r, F and P values of 0.848, 25.58 and <0.001 for CSF data, and the corresponding values of 0.815, 18.45 and 0.002 for brain data). The kinetic parameters determined by this graphic method for the distribution of indinavir to CSF and brain are listed in Table 2. The ER values calculated for CSF and brain again reflect the highly limited CNS entry of the drug.

Discussion

A series of in-vitro investigations based on cultured mammalian cells demonstrated the limited BBB permeability of HIV protease inhibitors, mainly due to the presence of P-gp in the plasma membrane of the brain vascular endothelial cells (Kim et al 1998; Lee et al 1998; Choo et al 2000). Although

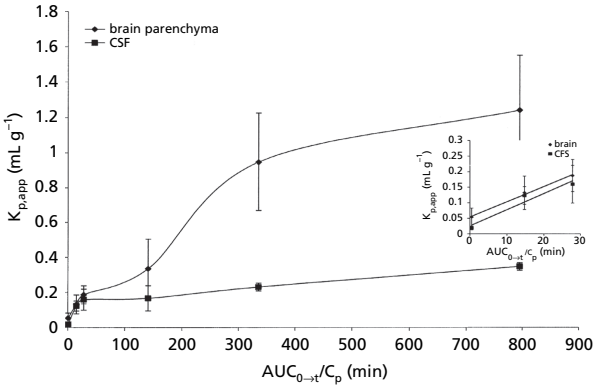

Figure 5 Graphic representation of the uptake of indinavir by rat brain parenchyma and cerebrospinal fluid (CSF) after intravenous administration of 5 mg kg^{-1} indinavir sulfate to male Sprague-Dawley rats (n = 4 for each time point). Inset: integration plot analysis of the uptake of indinavir by rat brain parenchyma and CSF after intravenous administration of 5 mg kg^{-1} indinavir sulfate to rats (n = 4 for each time point).

cell culture based models are useful tools for evaluation of the possible mechanisms of BBB transport as well as the factors influencing this process, the predictability of the actual in-vivo condition using these models is limited (Pardridge et al 1990; Megard et al 2002), mainly due to the overestimation of the actual BBB permeability by this method (Megard et al 2002).

A number of in-vivo models have been developed for the quantitative evaluation of the CNS transport of anti-HIV drugs (Anderson et al 1990; Galinsky et al 1990; Pardridge et al 1990; Takasawa 1997a, b; Kim et al 1998; Wu et al 1998; Megard et al 2002; Hamidi 2006a). In some of these models (Takasawa 1997a; Wu et al 1998; Hamidi 2006a), referred to as single-passage methods, the early stages of the brain/CSF exposure to drug, in which the drug influx is much greater than the efflux rate, is used for the determination of a clearance parameter. Another series of methods, known as multiple-passage methods (Anderson et al 1990; Galinsky et al 1990; Wang & Sawchuk 1995), involve the systemic administration of the drug to the animal and determination of the blood, CSF and brain concentration–time profiles over a considerably long time period (i.e. a full-course pharmacokinetic study), which ultimately results in determination of the influx/efflux rate constants. We combined the two above-mentioned methods in this study to use the relative advantages of both types of data analysis for extensive characterization of the CNS transport kinetics of indinavir in rat using the same set of data. Using this combinational approach, not only could a series of very useful kinetic parameters be estimated for CNS distribution of the drug, but also some invaluable information was collected regarding the mechanism of the drug transport to the CNS.

The indinavir concentration builds up and declines more slowly in the brain parenchyma than in the CSF (Figure 2). This observation can be explained by the slower diffusion of indinavir through the brain parenchyma and/or the presence of high-affinity binding site(s) for the drug in this tissue. The limited drug diffusion through the brain parenchyma is known (Fenstermacher & Kaye 1988), but whether the drug binds tightly to some brain component(s) remains to be evaluated. In contrast, the relatively faster build up and decline rate of CSF concentrations of the drug is attributable to the homogenous liquid nature of this tissue together with the high bulk flow rate of this fluid (Habgood et al 2000). Comparing the t_{max} values of 5 and 60 min for indinavir in CSF and brain (Figure 2), it does not seem likely that the drug enters CSF via the brain parenchyma. Taking the higher K_{in} ($P < 0.001$) and K_{out} ($P < 0.001$) values of the drug in CSF compared with the brain parenchyma (more than 2-fold higher K_{in} and 10-fold higher K_{out} values; Table 2) into account, it seems possible that the influx and efflux of the drug into brain parenchyma occurs mainly via CSF. This theory is supported by the finding that the initial uptake clearance of indinavir by brain parenchyma compares with that of CSF ($P > 0.05$) (Table 2), which reflects the possibility of the presence of common routes for the drug influx to brain parenchyma and CSF. On the other hand, as mentioned earlier, the apparent K_{in} and K_{out} values estimated in this study for brain distribution of indinavir were not significantly different ($P > 0.05$). This observation seems somehow unrealistic considering the known active role of at least one efflux transporter, that is P-gp, in the BBB transport of indinavir (Kim et al 1998; Choo et al 2000; Megard et al 2002; Hamidi 2006b) and the limited inherent BBB permeability of the drug (Megard et al 2002). An explanation for the disagreement may be the involvement of CSF in the drug movements into/from the brain parenchyma, which causes the estimated apparent K values to deviate from their real values. Alternatively, the similar uptake clearance of indinavir by CSF and brain parenchyma could be explained by the presence of two independent, yet similar, routes for drug entry to these two compartments. Finally, the actual drug transport mechanism may be a combination of the two above-mentioned cooperative and independent mechanisms. Given the fact that there is free drug exchange between brain interstitial fluid and CSF across the ependymal surface (Fenstermacher et al 1981), the cooperative mechanism seems more likely than the independent one.

Since there are several carrier-mediated saturable mechanisms involved in drug transport between the blood circulation and CNS (Tsuji 2000), there is free drug movement between brain interstitial fluid and CSF (Fenstermacher et al 1981), and as the brain is a heterogenous tissue consisting of different components and intra-tissue sub-populations of cells, the validity of the assumptions made in this model is questionable. However, as with all mathematical models constructed for studies on physiological systems, we have to simplify the highly complex actual mechanisms involved. Particular care should be taken when interpreting the outputs of this model.

The elimination rate constant of indinavir from CSF exceeds the corresponding tissue uptake rate constant ($P < 0.001$; Table 2). This observation indicates the important contribution of the drug efflux in the limited overall CNS distribution of the drug. Since it has been shown that indinavir is a potential substrate for P-gp (Kim et al 1998; Choo et al 2000; Megard et al 2002; Hamidi 2006b), the higher K_{out} values of indinavir in CSF can be explained by the localization of this efflux transporter in BCSFB (Wijnholds et al 2000).

The brain K_{in} values of indinavir obtained in this study (Table 2), being indicative of limited brain entry of the drug, are much higher (about 20-fold) than the corresponding values estimated for zidovudine (Galinsky et al 1990) and 2′,3′-dideoxyinosine (Anderson et al 1990), which can be explained by the much higher octanol/water partition coefficient (PC) of 457 for indinavir (Johnson et al 1999) compared with the PC values of 0.055 and 0.11 reported for 2′,3′-dideoxyinosine (Anderson et al 1990) and zidovudine (Galinsky et al 1990), respectively. It has been found that the brain PS of a compound is a function of its PC and molecular weight (M_r) (Pardridge et al 1990; Abraham & Platts 2000). According to an in-vitro/in-vivo brain transport study (Pardridge et al 1990) using a wide variety of compounds with different physicochemical properties, the in-vivo PS of a compound from rat BBB relates to the PC and M_r values according to the formula: $\ln(PS\sqrt{M_r}) = 0.54\ (\ln PC) - 0.13$. Taking the PC (457) and M_r (613.8) of indinavir into consideration, the formula predicts a PS value of 0.36 mL min^{-1} g^{-1} for this drug, which is about 35-fold higher than the PS value estimated in this study (i.e. 1.05×10^{-2} mL min^{-1} g^{-1}). The difference between the observed and predicted values of brain PS of indinavir can be explained by the steric hindrance owing to the molecular structures of the lipid-mediated transport pathways, sequestration by the constituents of BBB (Pardridge et al 1990) and/or the first-pass metabolism of the drug by the endothelial cells (Anderson et al 1990). The limited in-vivo brain influx of indinavir despite the high predicted PS of the drug has been reported by Megard et al (2002).

Both the V_{vas} and V'_{vas} values estimated in this study (Table 2: 6 mL/100 g from full-course neuropharmacokenetic analysis and 9 mL/100 g from the initial uptake clearance approach) are significantly higher than the brain vascular plasma volumes estimated using different methods. This difference can be attributed to, firstly, the inherent method-dependent variations in reported values for V_{vas} in the literature (Bereczki et al 1992), such that a wide range of values from 0.7 mL/100 g (Smith et al 1988) to 2.5 mL/100 g (Todd et al 1992) or even about 5 mL/100 g (Sandor et al 1986) have been reported. The upper end of this range is around the estimated value in the present study. Secondly, the presence of some brain parenchymal regions devoid of BBB (Healy & Wilks 1993), thus freely accessible to indinavir without crossing BBB (Anderson et al 1990; Galinsky et al 1990), as well as sequestration of the drug by brain vascular tissue (Healy & Wilks 1993; Hargreaves & Pardridge 1988) may be responsible, at least in part, for this difference.

Conclusions

Collectively, the results of this study indicate that the net CNS transfer of indinavir is restricted because of both the limited influx and more efficient efflux of the drug, particularly in the case of CSF. This combinational model can be used for extensive evaluation of possible effects of different factors on the CNS distribution of the drugs (e.g. drug–drug interactions). Given the fact that the overall integrity of the BBB may be compromised as a result of HIV infection (Wiley et al 1986), application of the data obtained using this model for HIV-infected patients should be considered carefully. The model is currently being used in our laboratory for a drug–drug interaction study on indinavir.

References

Abraham, M. H., Platts, J. A. (2000) Physicochemical factors that influence brain uptake. In: Begley, D. J., Bradbury, M. W., Kreuter, J. (eds) *Blood-brain barrier and drug delivery to the CNS*. Marcel Dekker Inc., New York, pp 9–32

Acosta, E. P., Henry, K., Baken, L., Page, L. M., Fletcher, C. V. (1999) Indinavir concentrations and antiviral effect. *Pharmacotherapy* **19**: 708–712

Anderson, B. D., Hoesterey, B. L., Baker, D. C., Galinsky, R. E. (1990) Uptake kinetics of 2′,3′-dideoxyinosine into brain and cerebrospinal fluid of rats: intravenous infusion studies. *J. Pharmacol. Exp. Ther*. **253**: 113–118

Bereczki, D., Wei, L., Acuff, V., Gruber, K., Tajima, A., Patlak, C., Fenstermacher, J. (1992) Technique-dependent variations in cerebral microvessel blood volumes and hematocrits in the rat. *J. Appl. Physiol*. **73**: 918–924

Chiba, M., Hensleigh, M., Lin, J. H. (1997) Hepatic and intestinal metabolism of indinavir, an HIV protease inhibitor, in rat and human microsomes. Major role of CYP3A. *Biochem. Pharmacol*. **53**: 1187–1195

Chiba, M., Nishime, J. A., Neway, Y., Lin, Y., Lin, J. H. (2000) Comparative in vitro metabolism of indinavir in primates – a unique stereoselective hydroxylation in monkey. *Xenobiotica* **30**: 117–129

Choo, E. F., Leake, B., Wandel, C., Imamura, H., Wood, A. J., Wilkinson, G. R., Kim, R. B. (2000) Pharmacological inhibition of P-glycoprotein transport enhances the distribution of HIV-1 protease inhibitors into brain and testis. *Drug. Metab. Dispos*. **28**: 655–660

Crone, C. (1965) The permeability of brain capillaries to non-electrolytes. *Acta. Physiol. Scand*. **64**: 407–417

Erickson, J. W., Gulnik, S. V., Markowitz, M. (1999) Protease inhibitors: resistance, cross-resistance, fitness and the choice of initial and salvage therapies. *AIDS* **13** (Suppl. A): S189–S204

Eron, J. J. (2000) HIV-protease inhibitors. *Clin. Infect. Dis*. **30** (Suppl. 2): S160–S170

Fenstermacher, J., Kaye, T. (1988) Drug "diffusion" within the brain. *Ann. N. Y. Acad. Sci*. **531**: 29–39

Fenstermacher, J. D., Blasberg, R. G., Patlak, C. S. (1981) Methods for quantifying the transport of drugs across brain barrier systems. *Pharmacol. Ther*. **14**: 217–248

Galinsky, R. E., Hoesterey, B. L., Anderson, B. D. (1990) Brain and cerebrospinal fluid uptake of zidovudine (AZT) in rats after intravenous injection. *Life. Sci*. **47**: 781–788

Gulick, R. M., Mellors, J. W., Havlir, D., Eron, J. J., Gonzalez, C., McMahon, D., Richman, D. D., Valentine, F. T., Jonas, L., Meibohm, A., Emini, E. A., Chodakewitz, J. A. (1997) Treatment with indinavir, zidovudine, and lamivudine in adults with human immunodeficiency virus infection and prior antiretroviral therapy. *N. Engl. J. Med*. **337**: 734–739

Haas, D. W., Stone, J., Clough, L. A., Johnson, B., Spearman, P., Harris, V. L., Nicotera, J., Johnson, R. H., Raffanti, S., Zhong, L., Bergqwist, P., Chamberlin, S., Hoagland, V., Ju, W. D. (2000) Steady-state pharmacokinetics of indinavir in cerebrospinal fluid and plasma among adults with human immunodeficiency virus type 1 infection. *Clin. Pharmacol. Ther*. **68**: 367–374

Habgood, M. D., Begley, D. J., Abbott, N. J. (2000) Determination of passive drug entry into central nervous system. *Cell. Mol. Neurobiol*. **20**: 231–253

Hagendorff, A., Dettmers, C., Danos, P., Wetter, S., Lassau, M., Pizzulli, L., Omran, H., Bauer, T., Hartmann, A., Luderitz, B. (1994) Carotid artery stenosis and tachyarrhythmias: regional cerebral blood flow during high-rate ventricular pacing after one vessel occlusion in rats. *J. Clin. Invest*. **72**: 775–781

Hamidi, M. (2006a) Simple and sensitive high-performance liquid chromatography method for the quantitation of indinavir in rat plasma and central nervous system. *J. Sep. Sci*. **29**: 620–627

Hamidi, M. (2006b) Role of P-glycoprotein in tissue uptake of indinavir in rat. *Life Sci*. **79**: 991–998

Hargreaves, K. M., Pardridge, W. M. (1988) Neutral amino acid transport at the human blood-brain barrier. *J. Biol. Chem.* **263**: 19 392–19 397

Healy, D. P., Wilks, S. (1993) Localization of immunoreactive glutamyl aminopeptidase in rat brain. II. Distribution and correlation with angiotensin II. *Brain Res*. **606**: 295–303

Johnson, B. D., Howard, A., Varsolona, R., McCauley, J., Ellison, D. K. (1999). Indinavir sulfate. In: Brittain, H. G. (ed.) *Analytical profiles of drug substances and excipients*. Academic Press, San Diego, pp 319–358

Keep, R. F., Jones, H. C. (1990) A morphometric study on the development of the lateral ventricle choroid plexus, choroid plexus capillaries and ventricular ependyma in the rat. *Brain Res. Dev. Brain Res*. **56**: 47–53

Kim, R. B., Fromm, M. F., Wandel, C., Leake, B., Wood, A. J., Roden, D. M., Wilkinson, G. R. (1998) The drug transporter P-glycoprotein limits oral absorption and brain entry of HIV-1 protease inhibitors. *J. Clin. Invest*. **101**: 289–294

Krebs, F. C., Ross, H., McAllister, J., Wigdahl, B. (2000) HIV-I-associated central nervous system dysfunction. *Adv. Pharmacol. Res*. **19**: 315–385

Lee, C. G., Gottesman, M. M., Cardarelli, C. O., Ramachandra, M., Jeang, K. T., Ambudkar, S. V., Pastan, I., Dey, S. (1998) HIV-1 protease inhibitors are substrates for the MDR1 multidrug transporter. *Biochemistry* **37**: 3594–3601

Lin, J. H., Chiba, M., Balani, S. K., Chen, I. W., Kwei, G. Y., Vastag, K. J., Nishime, J. A. (1996) Species differences in the pharmacokinetics and metabolism of indinavir, a potent human immunodeficiency virus protease inhibitor. *Drug. Metab. Dispos*. **24**: 1111–1120

Martin, C., Sonnerborg, A., Svensson, J. O., Stahle, L. (1999) Indinavir-based treatment of HIV-1-infected patients: efficacy in the central nervous system. *AIDS* **13**: 1227–1232

Megard, I., Garrigues, A., Orlowski, S., Jorajuria, S., Clayette, P., Ezan, E., Mabondzo, A. (2002) A co-culture-based model of human blood-brain barrier: application to active transport of indinavir and in vivo-in vitro correlation. *Brain. Res*. **927**: 153–167

Ohno, K., Pettigrew, K. D., Rapoport, S. I. (1978) Lower limits of cerebrovascular permeability to nonelectrolytes in the conscious rat. *Am. J. Physiol*. **235**: H299–H307

Pardridge, W. M., Triguero, D., Yang, J., Cancilla, P. A. (1990) Comparison of in vitro and in vivo models of drug transcytosis through the blood-brain barrier. *J. Pharmacol. Exp. Ther*. **253**: 884–891

Pialoux, G., Fournier, S., Moulignier, A., Poveda, J. D., Clavel, F., Dupont, B. (1997) Central nervous system as a sanctuary for HIV-1 infection despite treatment with zidovudine, lamivudine and indinavir. *AIDS* **11**: 1302–1303

Renkin, E. M. (1959) Transport of potassium-42 from blood to tissue in isolated mammalian skeletal muscle. *Am. J. Physiol*. **197**: 1205–1210

Sandor, P., Cox-van Put, J., deJong, W., de Wied, D. (1986) Continuous measurement of cerebral blood volume in rats with the photoelectric technique: effect of morphine and naloxone. *Life Sci*. **39**: 1657–1665

Shargel, L., Yu, A. B. C. (1999) *Applied biopharmaceutics and pharmacokinetics*. Appleton & Lange, Stamford

Smith, Q. R., Ziylan, Y. Z., Robinson, P. J., Rapoport, S. I. (1988) Kinetics and distribution volumes for tracers of different sizes in the brain plasma space. *Brain Res*. **462**: 1–9

Takasawa, K., Terasaki, T., Suzuki, H., Ooie, T., Sugiyama, Y. (1997a) Distributed model analysis of 3′-azido-3′-deoxythymidine and 2′,3′-dideoxyinosine distribution in brain tissue and cerebrospinal fluid. *J. Pharmacol. Exp. Ther*. **282**: 1509–1517

Takasawa, K., Terasaki, T., Suzuki, H., Sugiyama, Y. (1997b) In vivo evidence for carrier-mediated efflux transport of 3′-azido-3′-deoxythymidine and 2′,3′-dideoxyinosine across the blood-brain barrier via a probenecid-sensitive transport system. *J. Pharmacol. Exp. Ther*. **281**: 369–375

Tatsuta, T., Naito, M., Oh-hara, T., Sugawara, I., Tsuruo, T. (1992) Functional involvement of P-glycoprotein in blood-brain barrier. *J. Biol. Chem*. **267**: 20 383–20 391

Todd, M. M., Weeks, J. B., Warner, D. S. (1992) Cerebral blood flow, blood volume, and brain tissue hematocrit during isovolemic hemodilution with hetastarch in rats. *Am. J. Physiol*. **263**: H75–H82

Tsuji, A. (2000) Specific mechanisms for transporting drugs into brain. In: Begley, D. J., Bradbury, M. W., Kreuter, J. (eds) *Blood-brain barrier and drug delivery to the CNS*. Marcel Dekker Inc., New York, pp 121–144

van der Sandt, I. C., Vos, C. M., Nabulsi, L., Blom-Roosemalen, M. C., Voorwinden, H. H., de Boer, A. G., Breimer, D. D. (2001) Assessment of active transport of HIV protease inhibitors in various cell lines and the in vitro blood-brain barrier. *AIDS* **15**: 483–491

Wang, Y., Sawchuk, R. J. (1995) Zidovudine transport in the rabbit brain during intravenous and intracerebroventricular infusion. *J. Pharm. Sci*. **84**: 871–876

Waynforth, H. B., Flecknell, P. A. (1992) *Experimental and surgical techniques in rat*. Academic Press, London

Wijnholds, J., deLange, E. C., Scheffer, G. L., van den Berg, D. J., Mol, C. A., van der Valk, M., Schinkel, A. H., Scheper, R. J., Breimer, D. D., Borst, P. (2000) Multidrug resistance protein 1 protects the choroid plexus epithelium and contributes to the blood-cerebrospinal fluid barrier. *J. Clin. Invest*. **105**: 279–285

Wiley, C. A., Schrier, R. D., Nelson, J. A., Lampert, P. W., Oldstone, M. B. (1986) Cellular localization of human immunodeficiency virus infection within the brains of acquired immune deficiency syndrome patients. *Proc. Natl. Acad. Sci. USA* **83**: 7089–7093

Wu, D., Clement, J. G., Pardridge, W. M. (1998) Low blood-brain barrier permeability to azidothymidine (AZT), 3TC, and thymidine in the rat. *Brain. Res*. **791**: 313–316